https://doi.org/10.30799/jnst.195.19050102 J. Nanosci. Tech. - Volume 5 Issue 1 (2019) 584–586

ISSN: 2455-0191

Share Your Innovations through JACS Directory

Journal of Nanoscience and Technology

Visit Journal at http://www.jacsdirectory.com/jnst

One Step Hydrothermal Synthesis of Nanostructured VO_2(B) for Photocatalytic Application

Meenu, Pawan Kumar, Brijnandan S. Dehiya*

Nanostructured Materials Laboratory, Department of Materials Science and Nanotechnology, Deenbandhu Chhotu Ram University of Science & Technology, Murthal, Sonepat – 131 039, Haryana, India.

ARTICLEDETAILS

Article history:
Received 19 December 2018
Accepted 29 December 2018
Available online 05 January 2019

Keywords:
Hydrothermal Method
Photocatalysis
VO_2(B)

ABSTRACT

This paper reports the one step hydrothermal synthesis of VO_2(B) at high temperature in 24 h by using citric acid monohydrate as reducing agent and vanadium pentoxide as vanadium source. The phase of synthesized material is confirmed by XRD and indexed by JCPDS card. XRD results favors for pure phase of VO_2(B). For confirmation of chemical composition vibrational bands FTIR is performed. For finding optical band gap, Tauc calculation has be done from UV-Vis spectroscopy. Photocatalytic activity is performed under UV radiation for 180 min. SEM and EDX is also performed for morphology and confirmation of elemental composition.

1. Introduction

Different polymorph phases of V-O systems with VO_2 (A) [1], VO_2 (B) [2], VO_2 (C) [3], VO_2 (D) [4], VO_2 (M) [5, 6], VO_2 (R) [7] and VO_2 (Paramontroseite) [8]. Among all vanadium dioxide phases, VO_2 (B) and VO_2 (M) are very interesting due to their layered structure, good energy capacity with high work potential and promising applications in the field of energy conversation [9, 10]. VO_2 (B) is used as cathode material for Li-ion batteries not only due to its electrode potential, but also due to two edges- sharing octahedra units and form a tunnel like structure, through which Li-ions can exchange easily [11]. VO_2 (B) is also used as precursor for synthesis of VO_2 (M/R) [12]. VO_2 (B) can also be used for dye degradation. Till now very few works are reported on this. VO_2 (M) is thermochromic material which shows reversible first-order phase transition near to room temperature which makes it useful for practical applications.

In this paper, VO_2 (B) is obtained by taking an optimum molar ratio of vanadium source to reducing agent via hydrothermal method. Here vanadium source is taken vanadium penta oxide and reducing agent, citric acid monohydrate is taken.

2. Experimental Methods

2.1 Materials and Method

Vanadium pentoxide (V_2O_5, Sigma Aldrich) as vanadium source and citric acid monohydrate ($C_6H_8O_7.H_2O$, Sigma Aldrich) as reducing agent were used as reactants. First of all, 5 mmol V_2O_5 was dissolved in 40 mL of deionized water. The mixture was stirred for 15 minutes using a magnetic stirrer at 60 °C. Then, 15 mmol citric acid monohydrate ($C_6H_8O_7.H_2O$) was added to the solution and stirring was prolonged for 20 more minutes. The resultant yellow aqueous solution was turned in to blue clear solution which was transferred into a 60 mL stainless steel autoclave with Teflon lined cup, then sealed and kept in an oven which was preheated to 230 °C. The autoclave was kept at that temperature for 24 h. After this reaction process, the autoclave was left for cooling to room temperature overnight. The following day, the dark blue/black precipitate was obtained. The precipitate was washed with deionized water and ethanol several times to maintain a pH value, and then filtered and dried in an oven at 60 °C for 24 h. Finally, after crushing in an agate mortar pestle, a dark blue/black powder was obtained.

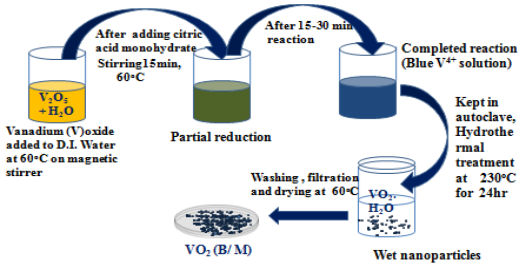

Fig. 1 Complete reduction process during synthesis of VO_2 via hydrothermal reaction

2.2 XRD Analysis

The phase of synthesized material was confirmed by XRD (Rigaku Ultima IV). The scanning angle was taken in between from 20 to 70 degree which give information regarding crystal structure of the prepared sample.

2.3 FTIR Analysis

This analysis was used to identify the presence of vibrational bonds between V-O system and for presence of functional group in the sample within the wavenumbers from 4000 cm^{-1} to 400 cm^{-1} by using Perkin Elmer Frontier FTIR. The spectra regarding FTIR give information which confirm the chemical composition of the synthesized sample.

2.4 SEM and EDX Analysis

For information regarding morphology of the prepared samples, Scanning Electron Microscope (SEM) (JEOL) was performed. For elemental scanning, SEM-EDX was performed which confirm the elemental composition of the synthesized material.

2.5 UV-VIS Spectroscopy

Optical properties were examined by UV-Vis spectrophotometer (UV-2401 PC Shimadzu) and energy band gap of sample was found by using Tauc Plot which is obtained from UV-VIS graph by using the equation as:

$$(\alpha\hbar\nu) = A\,(\hbar\nu - Eg)^{n} \quad (1)$$

where α is the absorption coefficient with value 2.303 log (T/d) in which d is the thickness of sample and T is the Transmission, ħν is the photon energy, value of n depends on nature of transmission which is 1/2, 3/2, 2 and 3 for direct-allowed transition, for direct forbidden, for indirect

*Corresponding Author:drbrijdehiya.msn@dcrustm.org(Brijnandan S. Dehiya)

https://doi.org/10.30799/jnst.195.19050102

allowed and for indirect forbidden respectively. The value of energy band gap is found by taking the intercept of extrapolation to zero absorption with photon energy $(\alpha\hbar\nu)^2 = 0$.

2.6 Photocatalytic Activity

The photocatalytic properties of our samples were examined by monitoring the decomposition Rhodamine B (RhB) under by irradiation from Mercury (254 nm) lamp. For experiment, 10 ppm solution was made and in which volume of solution was taken 50mL and amount of adsorbent was taken 15 mg.

3. Results and Discussion

After investigation, it was found that VO_2 can be produced by varying the molar ratio of precursors using a hydrothermal method at high temperature. Fig. 2 shows X-ray diffraction patterns of the as-prepared samples, which reveal that the concentrations of the reducing agent affect the formation of VO_2 phase. As shown in Fig. 2, with molar ratio 1:1.5 corresponding to pure VO_2 (B) (JCPDS no. 65-7960) is obtained. No peak of V_2O_5 is obtained in XRD which indicates that V_2O_5 has been completely reduced into VO_2 (B) with molar concentration ratio of 1:1.5 (vanadium pentoxide to citric acid) at 230 °C.

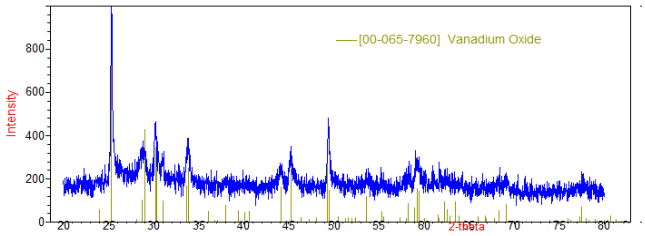

Fig. 2 XRD spectrum of synthesized sample

To investigate the chemical bonding between vanadium and oxygen ions, FTIR spectroscopy is performed. Figure 3 shows the FTIR spectrum of synthesized VO_2 samples prepared at reported hydrothermal condition. The main vibrational bands observed from the FTIR spectrum are at 534, 945, 1034 cm^{-1} and at higher values can be attributed to the various vibrational bands of V–O, O–H, and C–O bonds [13-16]. From the comparison with previous reports, bands nearly 534, 935 and 1034 cm^{-1} can be considered as intrinsic to vanadium oxide. From figure 3, it is observed that the main peaks due to different vanadium- oxygen systems are present: the initial broad vibrational band at 534 cm^{-1} is assigned to the ν(V–O–V) octahedral bending modes; the band at 945 cm^{-1} is attributed to the coupled vibration of ν(V=O) and ν(V–O–V); the band at 1045 cm^{-1} is attributed to the stretching of short ν(V–O) bonds that are also present in all curves.

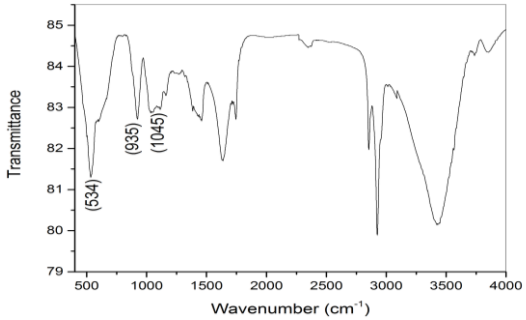

Fig. 3 FTIR spectrum of VO_2(B)with different vibrational bonds

The UV-Vis results show good absorbance in the UV-region and the energy absorption band gap was found with the help of a Tauc plot. The UV–visible spectrum of VO_2 (B) is shown in Fig. 4 obtained from as prepared samples. From the Fig. 4, it is observed that the absorbance is highest in UV-region and as we move towards the visible region, the absorbance decreases. The linear portions of the corresponding absorption coefficient data plot can be extrapolated to intersect the energy axes i.e. 'x' axis at α=0 [17]. The corresponding values of the energy data give the optical band gap of the synthesized samples.

The optical band gap is the minimum energy difference between the valance band and conduction band during electronic transition. The nature of electronic transition can be described by varying value of n. For direct allowed transition (n=1/2), optical band gap, E_g, is estimated from above plot, i.e. 3.25 eV as shown in Fig. 5.

Fig. 6 shows the morphology of the vanadium dioxide which is made of agglomerated particles. With this SEM-EDX is shown in which elemental composition of the material is shown which confirm the synthesis of VO_2. The ratio of elemental composition Table 1 is also shown which is in favor of XRD results.

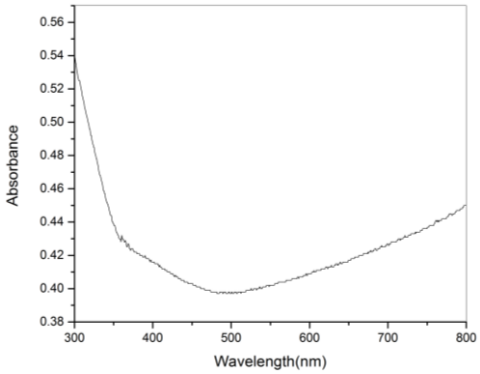

Fig. 4 UV-VIS spectrum for synthesized material

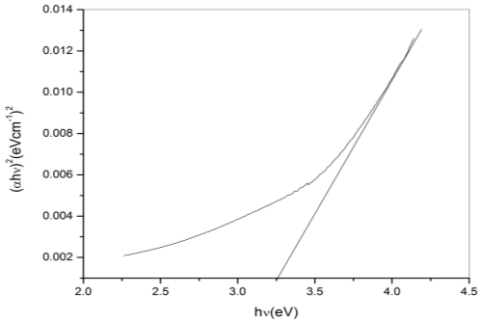

Fig. 5 Tauc Plot for VO_2 (B)

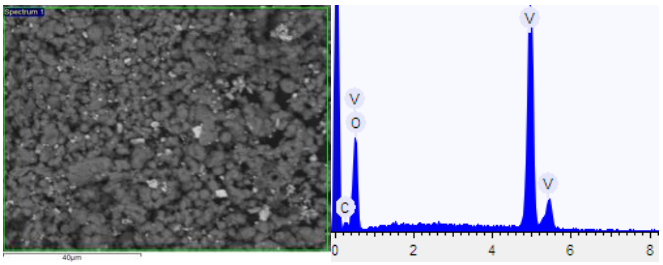

Fig. 6 SEM and EDX of vanadium dioxide as prepared materials

Table 1 Elemental composition of the material

Element	Weight %	Weight % σ	Atomic %
Oxygen	38.316	2.022	66.418
Vanadium	61.684	1.920	33.582

For photocatalytic degradation process, when premixed solution of VO_2(B) and RhB is illuminated with light of enough amount (sunlight or UV/Vis light source), the electron get excited and jump from valance band to conduction band, thus leaves a hole in valance band. The genereted hole combine with water and OH^- radical will produce. Similarly, electron will combine with O_2 and produce O_2^- radical. These generated radicals will take participate in photocatalytic degradation of RhB. Therefore, it is expected that the adsorption of RhB onto the VO_2 particles surface and adsorption ill take place on surface of material should be first step in the photocatalyst degradation mechanism. Further, the RhB ocuupied in both case on the surface of catalyst and then excited to generate hydroxyl radical and superoxide radical that both decomposed the adsorbed RhB. The whole photocatalyst degradation mechanism by VO_2(B) can be explained by following reactions:

$$VO_2 + RhB \leftrightarrow VO_2 - RhB \quad (1)$$

$$VO_2 - RhB + h\nu \leftrightarrow VO_2(e^-, h^+) - RhB \quad (2)$$

$$VO_2(h^+) + H_2O_{(ads)} \rightarrow VO_2(OH_{(ads)}\bullet) + H^+ \quad (3)$$

$$VO_2(h^+) + OH^-_{(ads)} \rightarrow VO_2(OH_{(ads)}\bullet) \quad (4)$$

$$VO_2(e^-) + O_{2\,(ads)} \rightarrow VO_2(O_2^-{}_{(ads)}\bullet) \quad (5)$$

$$OH_{(ads)}\bullet + RhB \rightarrow \text{intermediate products} + \text{mineral salt} \rightarrow CO_2 + H_2O \quad (6)$$

$$O_2{}^-{}_{(ads)}\bullet + RhB \rightarrow \text{intermediate products} + \text{mineral salt} \rightarrow CO_2 + H_2O \quad (7)$$

Reversible dye adsorption on the VO_2 surface is shown in Eq.(1). Eqs. (2)-(5) show the formation of OH free radical and superoxide free radical.

https://doi.org/10.30799/jnst.195.19050102

Eqs. (6) and (7) show OH free radical and superoxide free radical will attack the preadsorbed dye compound respectively. In Fig. 7, it is observed that pure VO_2(B), a transition metal oxide, degrades RhB upto 29% under the effect of UV radiation in 180min time. Decrease in absorption intensity with irridation time is indicating that degradation of oraganic pollutant RhB take place which means VO_2 is activewith efficiency i.e 29%, as shown in Fig. 8.

There following reasons are also responsible for the degradation effeciency : (1) band gap of VO_2 is in UV region that is why it active in this region; (2) d-orbital of vanadium can make V^{4+} ions interact directly with organic pollutant dye molecules, and the electron trapped by vanadium are transferred to the adsorbed O_2 to generate O_2^- radicals, which is benificial to react with the organics. Thus a wider spectrum, which activate VO_2 for dye degradation. Several basic factors also affect the photocatalytic process, such as light absorption, adsorption and contiminant molecules and the charge transformation and separation [56, 57].

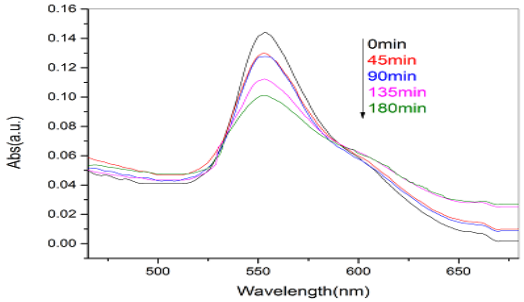

Fig. 7 Absorption spectrum of VO_2 (B)

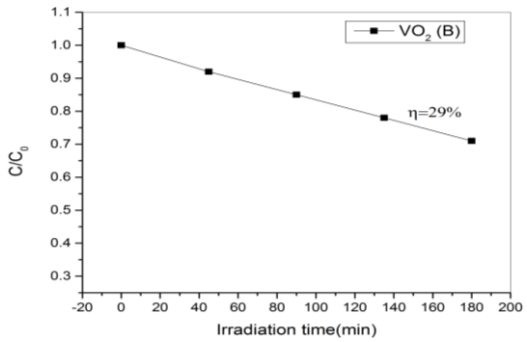

Fig. 8 Photocatalytic efficiency for VO_2 (B) with RhB in 180min

4. Conclusion

This paper represent the successful synthesis of VO_2(B) by hydrothermal technique at high temperature. XRD confirm the phase identification of the material. The morphology of synthesized material is observed by SEM and elemental composition is also confirmed by EDX. Physicochemical properties are studied by FTIR, UV-Vis spectroscopy. From Tauc plot calculation, it is observed that the band gap exist is UV-region which give information regarding a wide optical band gap. From these results, it can be observed that it may be photo catalytic active. Because a wide gap may increase the recombination time of electron and hole pair. The photocatalytic activity is observed to be 29% which give future scope for dye degradation. By making any new composite, it can be made useful for further photocatalytic applications.

References

[1] Y. Oka, S. Sato, T. Yao, N. Yamamoto, Crystal structures and transition mechanism of VO_2 (A), J. Solid State Chem. 598 (1998) 594-598.
[2] S.R. Popuri, Structurally restricted phase transitions in VO_2(B) and their impact on transport properties, J. Phys. Chem. C 119 (2015) 25085-25092.
[3] Z. Gui, R. Fan, X.H. Chen, Y.C. Wu, A new metastable phase of needle-like nanocrystalline VO_2·H_2O and phase transformation, J. Solid State Chem. 157 (2001) 250-254.
[4] L. Liu, New-phase VO_2 micro/nanostructures: investigation of phase transformation and magnetic property, New Jour. Chem. 36 (2012) 619-625.
[5] G. Andersson, J. Paju, W. Lang, W. Berndt, Studies on vanadium oxides, I. Phase Analysis, Acta Chem. Scand. 8 (1954) 1599-1606.
[6] B.L. Chamberland, New defect vanadium dioxide phases, J. Solid State Chem. 7 (1973) 377-384.
[7] D.B. McWhan, M. Marezio, J.P. Remeika, P.D. Dernier, X-ray diffraction study of metallic VO_2, Phy. Rev. B 10 (1974) 490-495.
[8] C. Wu, Z. Hu, W. Wang, M. Zhang, J. Yang, Synthetic paramontroseite VO_2 with good aqueous lithium-ion battery performance, Chem. Comm. 33 (2008) 3891-3893.
[9] G. Li, S. Pang, L. Jiang, Z. Guo, Z. Zhang, Environmentally friendly chemical route to vanadium oxide single-crystalline nanobelts as a cathode material for lithium-ion batteries, J. Phys. Chem. B 110 (2006) 9383-9386.
[10] C. Batista, R.M. Ribeiro, V. Teixeira, Synthesis and characterization of VO_2-based thermochromic thin films for energy-efficient windows, Nanoscale Res. Lett. 6 (2011) 301-308.
[11] I. Mjejri, N. Etteyeb, F. Sediri, Mesoporous vanadium oxide nanostructures: Hydrothermal synthesis, optical and electrochemical properties, Ceram. Int. 40 (2014) 1387-1397.
[12] Y. Zhang, VO_2(B) conversion to VO_2(A) and VO_2(M) and their oxidation resistance and optical switching properties, Mater. Sci. Poland 34 (2016) 169-176.
[13] F. Sediri, N. Gharbi, Nanorod B phase VO_2 obtained by using benzylamine as a reducing agent, Mater. Sci. Eng. B 139 (2007) 114-117.
[14] H. Ji, D. Liu, H. Cheng, C. Zhang, L. Yang, D. Ren, Infrared thermochromic properties of monoclinic VO_2 nanopowders using a malic acid-assisted hydrothermal method for adaptive camouflage, RSC Adv. 7 (2017) 5189-5194.
[15] S. Liang, Q. Shi, H. Zhu, B. Peng, W. Huang, One-step hydrothermal synthesis of W-Doped VO_2 (M) nanorods with a tunable phase-transition temperature for infrared smart windows, ACS Omega 1 (2016) 1139-1148.
[16] Y. Zhang, Controlled synthesis and electrochemical properties of vanadium oxides with different nanostructures, Bull. Mater. Sci. 35 (2012) 369-376.
[17] N.R. Mlyuka, R.T. Kivaisi, Correlation between optical, electrical and structural properties of vanadium dioxide thin films, J. Mater. Sci. 41 (2006) 5619-5624.
[18] L.W. Zhang, H.B. Fu, Y.F. Zhu, Efficient TiO_2 photocatalysts from surface hybridization of TiO_2 particles with graphite-like carbon, Adv. Funct. Mater. 18 (2008) 2180-2189.
[19] E. Solano Berral, Graphene composite for high photocatalyst application, Medicamenta 10 (1952) 215-224.

https://doi.org/10.30799/jnst.195.19050102

Cite this Article as: Meenu, Pawan Kumar, Brijnandan S. Dehiya, One step hydrothermal synthesis of nanostructured VO_2(B) for photocatalytic application, J. Nanosci. Tech. 5(1) (2019) 584–586.